

Cite this: *Chem. Sci.*, 2026, 17, 5510

All publication charges for this article have been paid for by the Royal Society of Chemistry

Received 24th September 2025
Accepted 4th January 2026

DOI: 10.1039/d5sc07429k

rsc.li/chemical-science

Chemo-enzymatic one-pot depolymerization of β -chitin

Joseph Brehm,^a Richard J. Lewis,^a Alan F. Scott,^{†b} David J. Morgan,^{ac} Thomas E. Davies,^a Nigel G. J. Richards^{ib*bd} and Graham J. Hutchings^{id*ac}

Decreasing our reliance on fossil carbon requires economically viable and scalable pathways to utilize sustainable sources, such as chitin. Current methods for converting chitin to high-value chemicals require treatment with strong acids and/or bases at high temperature, thereby giving complicated product mixtures with substantial, negative environmental impact. Here we present a chemo-enzymatic cascade in which H_2O_2 , generated *in situ* over Pd-based nanoalloys, is used by a lytic polysaccharide monooxygenase (LPMO) to convert chitin into soluble oligosaccharide fragments. Our approach, which minimizes oxidative damage to the enzyme, eliminates the need for atom-inefficient and energy intensive approaches to chitin depolymerization, potentially achieving substantial environmental and economic savings. The simplicity of this chemo-catalyst/enzyme cascade has significant advantages for accessing chitin as a bio-carbon resource.

Introduction

Currently, both chemical building blocks and energy are predominantly produced globally from fossil carbon sources (oil, natural gas, coal). Much emphasis has been placed on decarbonizing energy production and transportation, and major progress is being achieved in these areas through the expansion of renewable energy infrastructure and the electrification of transportation. Similarly, as part of achieving net zero targets,¹ urgent efforts are underway to defossilise industrial chemical production by exploiting alternate, sustainable, non-fossil carbon sources, such as biomass or “captured” CO_2 .^{2,3}

A considerable amount of success has already been reported in using lignocellulose,^{4,5} the most readily available sustainable form of carbon, as an industrial source of biofuel and high value chemicals, such as 5-hydroxymethylfurfural.⁶ Focus has therefore turned to developing sustainable chemical methods that exploit chitin,^{7,8} the second most abundant biopolymer on Earth with an estimated annual production of 10^{11} tonnes.⁹ Here progress has been slower because chitin, a relatively insoluble, crystalline biopolymer found in the exoskeletons of crustaceans and insects, is less chemically tractable.¹⁰ As

a result, existing industrial processing methods are energy intensive, require strong acids and/or bases, and generate toxic waste.⁷ A variety of technical challenges currently hamper development of economically viable, enzyme-based strategies to degrade chitin into chemically useful precursors on the industrial scale. For example, although chitinases can hydrolyse the β -1,4-glycosidic bonds connecting the *N*-acetylglucosamine monomers in chitin, these transformations are too inefficient for industrial usage when insoluble chitin is the substrate.¹¹ Moreover, bacterial and fungal chitobiasis can only remove *N*-acetyl-glucosamine from the non-reducing end of short, soluble chitin fragments.¹² These problems can, in principle, be overcome by using enzyme cocktails that include lytic polysaccharide monooxygenases (LPMOs);¹³ enzymes that catalyse the conversion of insoluble chitin into soluble oligosaccharides *via* an oxidative rather than hydrolytic mechanism.^{14–16} Strategies that employ mixtures of enzymes not only increase the cost of chitin breakdown but also complicate the development of optimized conditions (pH, temperature, concentration, *etc.*) to ensure that all of the components are active albeit with possibly reduced catalytic efficiencies. Perhaps the biggest drawback of using enzyme cocktails to break down chitin on an industrially viable scale, however, is the need to maintain LPMO activity over long timescales,¹⁴ especially when the oxidant is hydrogen peroxide (H_2O_2),¹⁷ a cheap reagent that is becoming increasingly used in biocatalysis.¹⁸ Numerous examples of H_2O_2 supply to per-oxy enzymes have been developed, with the continual addition of the preformed oxidant widely reported for multiple enzymatic systems.¹⁹ While effective, this approach leads to the continual dilution of product streams and the production of large quantities of contaminated aqueous waste. There are

^aMax Planck- Cardiff Centre on the Fundamentals of Heterogeneous Catalysis FUNCAT, Cardiff Catalysis Institute, School of Chemistry, Cardiff University, Cardiff CF24 4HQ, UK. E-mail: hutch@cardiff.ac.uk

^bSchool of Chemistry, Cardiff University, Cardiff CF10 3AT, UK

^cHarwellXPS, Research Complex at Harwell (RCaH), Didcot, OX11 0FA, UK

^dFoundation for Applied Molecular Evolution, Alachua, FL 32615, USA. E-mail: nrichards@ffame.org

[†] Present address: eXmoor pharma, Cell & Gene Therapy Centre, Britannia Road, Bristol BS34 5 TA, UK.



additional drawbacks associated with the means of industrial H_2O_2 production (*via* the Anthraquinone Oxidation Process), including atom-inefficiency, high energy and water requirements and considerable GHG release. We direct the reader to the work of Goor and colleagues for an in-depth review of industrial H_2O_2 production.²⁰

To address these concerns, several approaches to *in situ* H_2O_2 supply have been developed, including electrochemical, photocatalytic and multienzyme cascades. Enzymatic approaches,

perhaps represent the most well researched area, with H_2O_2 generation *via* glucose oxidase (GOx), formate oxidase (FOx), and choline oxidase (ChOx) widely reported.^{21,22,25} The operating conditions window of such approaches, however, is limited by the need to balance the stability and activity of multiple enzymatic components. Further drawbacks result from the stoichiometric production of undesirable by-products (*e.g.* gluconic acid in the case of GOx/glucose-mediated systems), which in turn necessitates continual pH control to maintain enzymatic performance.

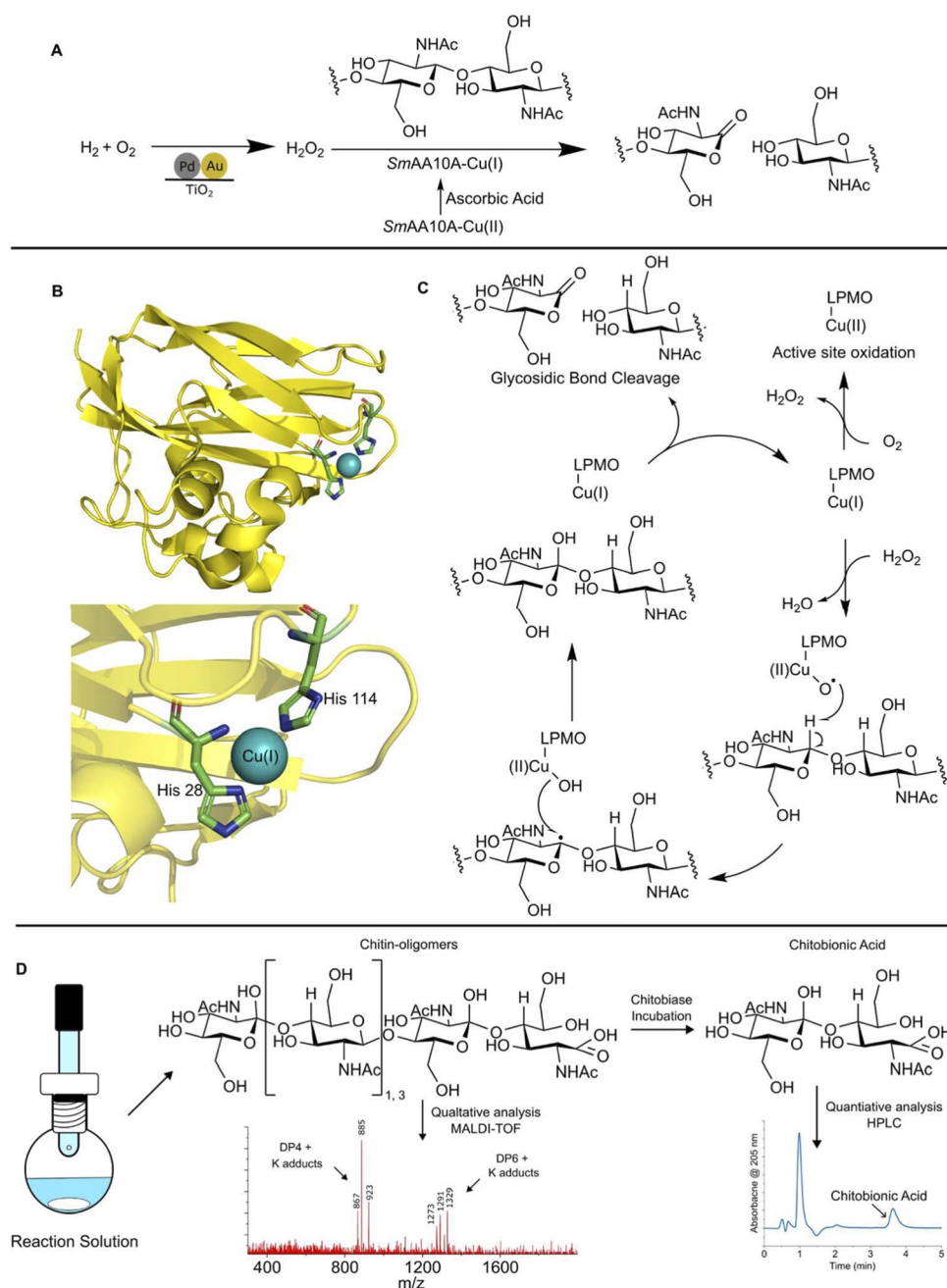


Fig. 1 Chemo-enzymatic cascade for β -chitin degradation. (A) Overall design of the 0.5%Au-0.5%Pd/TiO₂/smAA10A system to cleave the glycosidic bond by oxidation. (B) Schematic representation of smAA10A (PDB: 8RRY) showing the location of the Cu-binding site on the chitin-binding surface of the enzyme, and the histidine brace (His28 and His114).³³ (C) Catalytic mechanism of oxidative cleavage when H₂O₂ is the oxidant.³⁴ Note that ascorbate reduction to give Cu(I) is sub-stoichiometric. (D) Workflow for the qualitative (MALDI-TOF) and quantitative HPLC assays of chemo-enzymatic cascade activity.



Photocatalytic approaches to H_2O_2 supply suffer from similar drawbacks,^{23,24} relying on stoichiometric quantities of redox cofactors, and the formation of highly reactive oxygen-based radicals *via* irradiation of aqueous reaction media can lead to enzymatic deactivation and non-catalysed by-product formation. Finally, electrochemical H_2O_2 approaches, although effective, suffer from limited compatibility with existing reactor technologies.

We have reported a chemo-enzymatic approach to H_2O_2 supply, in which supported Pd-based species were coupled to a heme-dependent, unspecific peroxygenase enzyme (UPO) for selective C–H bond activation.²⁶ This approach overcomes the multiple concerns of the approaches discussed above, and is a practical, atom-efficient, and environmentally benign solution to supply continuous low concentrations of the oxidant to H_2O_2 -driven enzymatic processes. Building on these previous studies, which have focussed on selective chemical synthesis,^{27,28} we here turn our attention to the application of a chemo-enzymatic cascade for the multi-phase depolymerisation of β -chitin (derived from squid pens). We describe a system in which *in situ* H_2O_2 generation from H_2 gas and air, mediated by a well-studied 0.5%Au-0.5%Pd/TiO₂ chemo-catalyst²⁹ is coupled with a chitinolytic LPMO to fragment insoluble β -chitin (Fig. 1A). This approach has the advantage of eliminating the use of high initial H_2O_2 concentrations,^{30,31} which have been shown to oxidatively damage the metal-binding side chains of LPMOs (Fig. 1B); a process that leads to enzyme inactivation and low turnover numbers.^{17,32} Our system delivers increased levels of saccharification relative to those reported elsewhere, which are generally limited by the initial ascorbate concentration in the reaction mixture (Fig. 1C). Given its simplicity, our chemo-enzymatic strategy has potential for use in cost-effective β -chitin degradation on an industrial scale.

Results and discussion

We chose *Serratia marcescens* smAA10A (also known as CPB21)³⁵ as the chitinolytic LPMO in our chemo-enzymatic system for a number of reasons. Large quantities of the holo-enzyme are available by expression in *Escherichia coli* followed by incubation with CuSO_4 (Fig. S1 in SI). smAA10A has a strong preference for employing H_2O_2 rather than O_2 as an oxidant,³⁶ which permits completion of the catalytic cycle without the need for the addition of cellobiose dehydrogenase.³⁷ As importantly, smAA10A has a high binding affinity for β -chitin ($K_d = 1.4 \pm 0.4$ mM)³⁵ and retains activity in phosphate buffer at pH 6 ($k_{\text{cat}}/K_M \cong 10^5$ M⁻¹s⁻¹) (Fig. S2); conditions that are compatible with *in situ* H_2O_2 generation by the bimetallic AuPd/TiO₂ chemo-catalyst (Fig. S3).³⁸

In our experiments, β -chitin, chemo-catalyst, ascorbate, and the Cu(II)-containing holoenzyme were mixed in phosphate buffer, pH 6, in a sealed flask, under an atmosphere of air and H_2 , with the reaction initiated by stirring (Fig. S4). Under these conditions, ascorbate reduces the Cu(II) ion to give the active Cu(I)-containing holoenzyme, which uses the H_2O_2 generated *in situ* over the chemo-catalyst to cleave β -chitin into soluble chains of *N*-acetylglucosamine containing a single oxidized residue at the reducing end of the polysaccharide (Fig. 1D). We

highlight that the role of ascorbate is to reduce the resting Cu(II)–LPMO to the catalytically active Cu(I) state. Once primed, the LPMO operates through a peroxygenase mechanism in which H_2O_2 is the stoichiometric oxidant. As a result, the enzyme typically returns to the Cu(I) state after each catalytic turnover, so that additional ascorbate is only needed to counteract any adventitious oxidation to give Cu(II) in the active site. Therefore, ascorbate acts catalytically, not stoichiometrically, under these conditions of controlled H_2O_2 supply.³⁹ Each reaction was terminated by cessation of stirring and depressurizing the system at a defined timepoint, followed by filtration to remove insoluble β -chitin and the 0.5%Au-0.5%Pd/TiO₂ catalyst. Notably, no conversion of chitin was observed in the presence of the chemo-catalyst alone (Table S1). Further control experiments showed that the contribution of key reaction parameters to enzyme deactivation was minimal (Tables S2 and S3) and established improved system performance could be achieved through *in situ* supply of H_2O_2 compared to that offered by a purely O_2 -mediated pathway (Table S4). Mass spectrometry confirmed that oxidative cleavage occurred only at C-1 to give soluble oligosaccharide fragments, composed of 4, 6 and 8 residues (Fig. S5), as reported in earlier studies of smAA10A activity.^{17,40} This observation strongly supports the view that β -chitin oxidation is not occurring on the surface of the chemo-catalyst. Treatment of this oligosaccharide mixture with the enzyme chitobiase (ChB)¹² then gave *N*-acetylglucosamine and chitobionic acid (Figs. S6 and S7), which could be separated by chromatography and quantified (Fig. S8). The rate of LPMO-mediated oxidative cleavage could then be determined

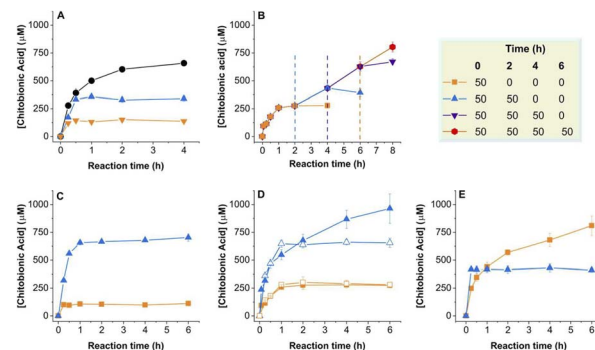


Fig. 2 Kinetics of chemo-enzymatic chitobionic acid formation from β -chitin. (A) Comparison of smAA10A activity with different sources of hydrogen peroxide in 50 mM $\text{K}_2\text{HPO}_4/\text{KH}_2\text{PO}_4$ buffer, pH 6 (10 mL) containing ascorbate (1 mM) and β -chitin (100 mg). (●) *In situ* H_2O_2 generation from H_2 gas and air by 0.5%Au-0.5%Pd/TiO₂ catalyst (0.01 g), (▲) drip fed H_2O_2 (252 nmol min⁻¹) and (▼) single injection of H_2O_2 (1 mM). (B) Effect of adding β -chitin to the chemo-enzymatic cascade at 0 h (■), 2 h (▲), 4 h (▼) and 6 h (●). Amounts of added β -chitin are shown in the accompanying table. (C) Effect of smAA10A concentration on the rate of chitobionic acid formation in the chemo-enzymatic cascade. (■) 0.25 mM, and (▲) 1 mM. (D) Effect of the amount of β -chitin (■) 5 mg mL⁻¹, and (▲) 20 mg mL⁻¹, or ascorbate (□) 0.5 mM and (△) 2 mM on the rate of chitobionic acid formation in the chemo-enzymatic cascade. (E) Effect of the amount of 0.5%Au-0.5%Pd/TiO₂ catalyst on the rate of chitobionic acid formation in the chemo-enzymatic cascade. (■) 0.05 mg mL⁻¹, (▲) 0.2 mg mL⁻¹. Reaction conditions are detailed elsewhere (see SI).



from the time-dependence of chitobionic acid production (Fig. 2A),^{36,40} and the extent of saccharification calculated based on quantitative measurements of *N*-acetyl-glucosamine and chitobionic acid concentrations (eqn S1 and S2).

Under our initial set of chemo-enzymatic conditions, β -chitin degradation proceeded with an initial rate corresponding to a turnover number (TON) of 1317, higher than that observed when *smAA10A* was incubated with β -chitin, ascorbate, and air in the same buffer under the same pressure (TON 1180) (Table S1). On the other hand, chitobionic acid production ceased after 4 h, reaching a plateau of approximately 650 mM in the presence of the 0.5%Au-0.5%Pd/TiO₂ catalyst (Fig. 2A). As a result, only approximately 7% of the β -chitin was converted into soluble polysaccharide fragments under these conditions. Control experiments ruled out the possibility that the plateau in chitobionic acid production was associated with cessation of chemo-catalytic H₂O₂ production due to “poisoning” of the chemo-catalyst surface by β -chitin, *smAA10A*, or ascorbate (Fig. S9). We note, however, that the stability of ascorbate is reduced in the presence of the chemo-catalyst (Fig. S10), which may influence the operation of any system at-scale. This observation is particularly important if a standing concentration of ascorbic acid is required to counteract occasional oxidation of Cu centres and suggests that the levels of this reductant may require continuous monitoring in any industrial process.

Alternatively, large-scale chitin degradation using this chemo-enzymatic strategy may require replacing ascorbate by well-studied alternative reducing agents.^{41,42} As such, we attributed the cessation of oxidative activity to a lack of available soluble substrate, competition between the oligosaccharide products and β -chitin for the enzyme, or *smAA10A* inactivation due to oxidative damage by H₂O₂, as discussed previously by Kuusk *et al.*³⁶ We were unable to demonstrate the effects of product inhibition for a variety of technical reasons (See SI) and so investigated whether the enzyme had become inactivated. The addition of β -chitin (50 mg amounts) to reaction mixtures in which chitobionic acid production had ceased, followed by re-pressurization, restored activity, albeit at a lower rate (Fig. 2B). This effect, which was not seen in similar “top up” experiments in which additional ascorbate or *smAA10A* was introduced into the system after 2 h (Fig. S11), was relatively short-lived, however, with the chitobionic acid concentration plateauing after only 2 h of reaction. Increasing the initial enzyme concentration did not significantly impact the initial rate of chitobionic acid production or the time at which apparent oxidative activity stopped (Fig. 2C) for a fixed quantity of β -chitin. Increasing the initial amount of β -chitin did, however, extend the time over which chitobionic acid was produced (Fig. 2D). Notably, the ability of β -chitin to protect against enzyme inactivation in our system is consistent with prior observations made under steady-state conditions.³⁶

β -Chitin breakdown depends on the method of H₂O₂ introduction

We next examined how *smAA10A* activity depended upon the method by which the H₂O₂ was introduced into the reaction

mixture (Fig. 2A). Thus, we determined the rate at which H₂O₂ was being introduced into the system due to the presence of the 0.5%Au-0.5%Pd/TiO₂ catalyst. These measurements showed a correlation between the amounts of chitobionic acid produced (Fig. 2A) and H₂O₂ produced by the chemo-catalyst, suggesting that oxidative activity is limited by chemo-catalytic supply of H₂O₂ in our chemo-enzymatic system. In consequence, the steady state concentration of H₂O₂ must be very low under our conditions; a prediction confirmed by our failure to detect residual H₂O₂ in solution, at least above 8.8 mM, when the chemo-enzymatic reaction was stopped. These experiments also showed that the rate of H₂O₂ production was approximately 252 nmol min⁻¹ under our conditions. Adding 1 mM H₂O₂ to a reaction mixture, as a single injection, in the absence of the chemo-catalyst resulted in chitobionic acid production at the same initial rate as seen for the complete chemo-enzymatic system (Fig. 2A). However, oxidative activity ceased after only a few minutes, presumably because of the sensitivity of *smAA10A* to H₂O₂ even at mild concentrations.³⁶ We then used a pump to introduce H₂O₂ into the reaction mixture at a rate of 252 nmol min⁻¹ (*i.e.* at a rate equivalent to that generated by our chemo-catalyst) (Fig. S12). Remarkably, chitobionic acid production under these conditions ceased after 0.5 h, although again, the initial rate was similar to that seen for the complete chemo-enzymatic system (Fig. 2A). This difference in behaviour was unexpected and may reflect the relatively slow stirring rate (250 rpm) due to the presence of solid β -chitin. Thus, the lack of rapid mixing may result in “hot spots” of elevated H₂O₂ concentration during addition, which can damage the enzyme. However, enzyme deactivation by the proprietary stabilizers, often acids,⁴³ found in commercial H₂O₂ cannot be ruled out.

This sensitivity of *smAA10A* activity to H₂O₂ concentration had been established in earlier work using glucose oxidase⁴⁴ and air to vary the rate of H₂O₂ generation.³⁶ We therefore investigated the effect of lowering the chemo-catalyst concentration on chitobionic acid formation and observed no cessation of enzyme activity at periods of up to 6 h when only 0.05 mg of 0.5%Au-0.5%Pd/TiO₂ (a 4-fold reduction) was present in the reaction mixture (Fig. 2E). Although this finding was consistent with the need for carefully controlling the rate of H₂O₂ generation, it was possible that enzyme inactivation might also be associated with metal leaching from the chemo-catalyst. Control experiments, however, established that metal leaching from the catalyst was exceptionally low under our chemo-enzymatic conditions, even at extended reaction times (Table S5). Moreover, the addition of homogeneous metals, in the form of metal chlorides (Table S6), did not substantially interfere with the ability of *smAA10A* to cleave β -chitin. Indeed, we further observed the relative stability of the system over successive runs (Table S7). Cumulatively, these experiments reveal the stability of *smAA10A* to leached metal species but indicate the need for further optimization of the chemo-catalyst to improve stability if this approach is to be operated effectively at scale.

Optimising the chemo-enzymatic breakdown of β -chitin

Having established that the rate of H₂O₂ synthesis must be carefully controlled in our chemo-enzymatic system, we set about



optimizing the conditions for *smAA10A*-catalyzed β -chitin over a 96-hour time period (Fig. 3). These experiments also required us to determine the rate of *smAA10A*-catalyzed cleavage of β -chitin when O_2 was the oxidant because of the possibility that very low amounts of 0.5%Au-0.5%Pd/TiO₂ chemo-catalyst might produce H₂O₂ sufficiently slowly so as to permit the LPMO to switch oxidants. In the absence of the chemo-catalyst, the LPMO proved to be active over an extended time period although, as expected, with the amount of chitobionic acid produced was limited by the initial ascorbate concentration (Fig. 3A). As a result, only 10.3% of β -chitin was saccharified (TON 1843) after 96 h under our conditions (Fig. 3B). The initial rate of β -chitin oxidation under these conditions was similar to that seen when the chemo-catalyst was present in amounts greater than, or equal to, 0.075 mg; these quantities also resulted in cessation of oxidative cleavage after 24 h of incubation (Fig. 3A). On the other hand, the initial rate of chitobionic acid production was greatly increased when we used either 0.025 or 0.05 mg of 0.5%Au-0.5%Pd/TiO₂ chemo-catalyst, with oxidative activity persisting for up to 96 h. In addition, the amount of chitobionic acid formed in the assay exceeded the initial concentration of ascorbate (1 mM) in both these chemo-enzymatic systems showing that *in situ* H₂O₂ was driving the saccharification reaction (Fig. 3A). Importantly, our simple chemo-catalyst/enzymatic cascade achieved 36% saccharification (TON 6372) after 96 h of incubation (Fig. 3B), which compares well with values reported for significantly more complicated mixtures used in LPMO-catalysed β -chitin degradation.^{42,45–47} Indeed, the chemo-enzymatic approach can be considered competitive with a range of enzymatic and purely chemical approaches to chitin depolymerisation (Tables S8 and S9).

The dynamic nature of the chemo-enzymatic system

Given our earlier observations upon use in the cascade system, which revealed the minor loss of active metals from the chemo-catalyst surface (Table S5), we were particularly interested in understanding the stability of the disparate metal species upon

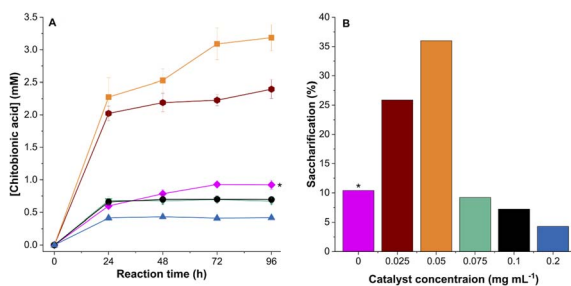


Fig. 3 Kinetics of β -chitin degradation by the chemo-enzymatic cascade over a 96-hour period. (A) Effect of the amount of chemo-catalyst on the rate of chitobionic acid formation. (\blacklozenge) 0 mg mL⁻¹ (*air is the oxidant in the absence of the 0.5%Au-0.5%Pd/TiO₂ catalyst), (\bullet) 0.025 mg mL⁻¹, (\blacksquare) 0.05 mg mL⁻¹, (\blacktriangledown) 0.075 mg mL⁻¹, (\bullet) 0.1 mg mL⁻¹ and (\blacktriangle) 0.2 mg mL⁻¹ of the 0.5%Au-0.5%Pd/TiO₂ catalyst. (B) Dependence of saccharification on the amount of 0.5%Au-0.5%Pd/TiO₂ catalyst after 96 h. Reactions were run under H₂ gas (1.6 bar) and air (0.4 bar) in 50 mM K₂HPO₄/KH₂PO₄ buffer, pH 6, (10 mL) containing *smAA10A* (0.5 mM), ascorbate (1 mM), and β -chitin (10 mg mL⁻¹).

exposure to chemo-enzymatic conditions. As expected given the wet co-impregnation route to catalyst synthesis, STEM-HAADF and XEDS (Fig. 4A and S13–S15), analysis of the as-prepared 0.5%Au-0.5%Pd/TiO₂ catalyst revealed the presence of a relatively wide particle size range, with much of the metal present as intermediate 5–15 nm nanoparticles or larger (>50 nm) species in addition to smaller (<1 nm) clusters.

XEDS mapping studies, confirmed that both the intermediate and larger species exist as AuPd alloys, while the smaller clusters were found to consist of Pd-only. In addition, although Au remains in the metallic state, surface domains of mixed Pd species (Pd⁰ and Pd²⁺) were observed by X-ray photoelectron spectroscopy, despite the exposure of the catalyst to reductive thermal treatment, which is in keeping with the known ability of Au to dictate the electronic state of Pd (Fig. S16).⁴⁸ STEM-HAADF and XEDS elemental analysis of chemo-catalyst recovered after use in the *smAA10*-mediated β -chitin cleavage reaction (Fig. 4B and S17) revealed that the larger AuPd alloys were stable under reaction conditions. However, we also observe the formation of a new population of smaller (<5 nm) Pd-only particles, presumably resulting from the agglomeration of the Pd-only clusters observed in the as-prepared material; notably these clusters were found to be absent in the case of the spent catalyst.

At extended reaction times (Fig. 4C and S18), the larger (>5 nm) AuPd nanoalloys are retained although there is a clear loss of the Pd-only species which cannot be correlated with metal leaching (Table S5) and implies the further agglomeration of Pd-only species. Importantly, these findings highlight the dynamic nature of the immobilised metals under the relatively complex reaction conditions and suggest the presence of a changing population-activity hierarchy, particularly at shorter reaction times under which Pd-only and AuPd species are both observed, and align well with comparative studies within the H₂O₂ direct synthesis literature.⁴⁸ Clearly, deconvoluting the contributions of individual populations to H₂O₂ synthesis would aid in improving overall cascade efficiency by kinetic balancing of individual reaction pathways. This is, however,

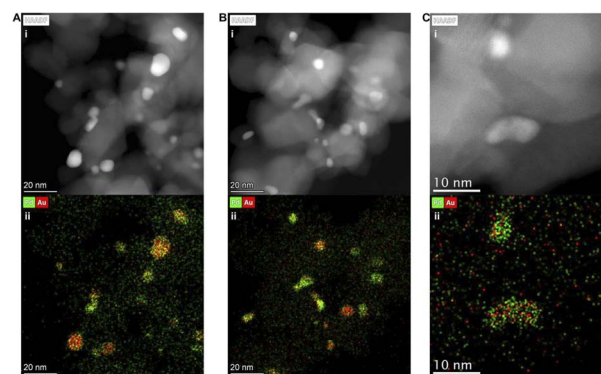


Fig. 4 Microstructural characterization of the 0.5%Au-0.5%Pd/TiO₂ catalyst. HAADF-STEM (top) and corresponding EDX (bottom) images of the chemo-catalyst when (A) freshly prepared, (B) used in β -chitin degradation for 2 h, and (C) used in β -chitin degradation for 96 h. Additional data are provided in the SI (Fig. S13–S15).



only one of several critical factors that must be considered when seeking to optimise chemo-enzymatic transformations.⁴⁹ Regardless, given the high stability of the bimetallic sites compared to the Pd-only analogues, our observations support a key role for the AuPd species in dictating cascade performance. XPS measurements also suggest that all surface Pd is rapidly reduced after exposure of the chemo-catalyst to the chemo-enzymatic conditions and further implicates Pd⁰ as the key species responsible for the catalysis (Fig. S16). This is particularly noteworthy given the debate surrounding the role of Pd speciation in H₂O₂ direct synthesis,^{50,51} with Pd⁰ species often demonstrating higher reactivity but lower selectivity towards H₂O₂ than Pd²⁺ analogues, primarily because of competitive degradation pathways. While such considerations may direct development of chemo-catalytic formulations that are highly selective toward H₂O₂, it is true that the rate of enzymatic utilisation often exceeds that of chemo-catalytic degradation. We therefore recommend that future studies focus on identifying catalyst formulations that are highly active toward H₂O₂ synthesis, with the caveat that the H₂O₂ production rate does not exceed that of its subsequent utilization.

Conclusions

At present, H₂O₂ is manufactured industrially using an indirect process that relies on the sequential reduction and re-oxidation of quinone carriers.⁵² Although highly effective, this production method is typically centralized and entails numerous energy-intensive distillation steps in order to raise H₂O₂ concentration prior to shipping, thereby minimizing transportation costs. More importantly, perhaps, the process is “atom inefficient” because over-hydrogenation of the quinone carrier necessitates continual replacement of this reagent. Finally, the addition of acid and halide stabilizing agents to prevent H₂O₂ degradation during transport and storage, which can limit catalyst stability, decrease reactor lifetime through corrosion, and generate substantial costs associated with their removal from product streams.⁵³ All of these factors are driving the development of alternative technologies for exploiting H₂O₂ in several industrially relevant processes. Indeed, eliminating the use of preformed, commercial H₂O₂ will result in significant economic savings and reduced greenhouse gas emissions.

Our chemo-enzymatic strategy therefore meets a number of criteria for realizing development of commercially viable methods to use LPMOs as reagents for the direct breakdown of β-chitin. First, we are able to optimize oxidative β-chitin cleavage while minimizing damage to the LPMO through control of H₂O₂ synthesis rates. Second, by merely varying the amount of chemo-catalyst we can optimize oxidative β-chitin cleavage while minimizing damage to the LPMO. Of course, this approach has been discussed previously using catalase as a means of controlling the rate of *in situ* H₂O₂ production, but this approach requires a level of control of enzyme concentration that may be impractical on large scale.⁵⁴ In contrast, H₂O₂ formation in our system could easily be controlled by changing the hydrogen flow rate. Equally, *in situ* H₂O₂ formation using multi-enzyme cocktails, such as glucose oxidase,^{36,48} is atom

inefficient and requires the inclusion of secondary substrates in stoichiometric amounts, thereby further complicating isolation of the desired *N*-acetylglucosamine product. We have also demonstrated the disadvantages of continually supplying low concentrations of commercial H₂O₂ to the LPMO in our system, both in terms of oxidation rate and enzyme inactivation that takes place over extended reaction times due to formation of ‘hot spots’ of locally high H₂O₂ concentration (Fig. 2A). Mitigating this problem by using dilute H₂O₂ feedstocks has clear drawbacks associated with the continual dilution of product streams and downstream purification.

Our work opens up a new avenue for successfully using chitin as a sustainable carbon source for the production of saccharides. Coupling an LPMO with a chemo-catalyst to deliver H₂O₂ as an oxidant is the key to this advance (Fig. 1A) because we can readily overcome the known sensitivity of this enzyme to oxidation without the introduction of extraneous reagents, such as *l*-glucose. The simplicity of this chemo-enzymatic system also facilitates the maintenance of LPMO activity merely by altering the amount of chemo-catalyst. It is clear that further work is needed to evaluate the efficacy of this chemo-enzymatic system for degrading less processed, mixed biopolymers and product mixtures resulting from up-stream chemical hydrolysis steps. On the other hand, although we only demonstrate the advantages of this system at the laboratory scale, this simple strategy has considerable potential for future deployment at scale.

Author contributions

N. G. J. R. and G. J. H. conceived the design of the study; J. B., A. F. S. and R. J. L. performed enzyme expression, assay development, and data analysis; J. B. and R. J. L. performed catalyst synthesis, testing, and data analysis; D. J. M. and T. E. D. conducted catalyst characterization and corresponding data processing; R. J. L., N. G. J. R. and G. J. H. provided technical advice and aided in the interpretation of results; J. B., R. J. L., N. G. J. R. and G. J. H., wrote the manuscript and SI, with subsequent review and editing by all other authors.

Conflicts of interest

There are no conflicts to declare.

Data availability

The data supporting this article have been included as part of the supplementary information (SI). Supplementary information: experimental procedures, Figs. S1–S18, Tables S1–S9 and supplementary references. See DOI: <https://doi.org/10.1039/d5sc07429k>.

Acknowledgements

We acknowledge the Protein Engineering and Proteomics Group, Department of Chemistry, Biotechnology and Food Science, Norwegian University of Life Sciences for generously providing a pET-30Xa/LIC vector harbouring the chitinase



gene. This work was supported by the Engineering and Physical Sciences Research Council, UK (EP/V014048/1). The authors also thank the Max Planck Centre for Fundamental Heterogeneous Catalysis (FUNCAT) and Cardiff University for additional support. XPS data collection was performed at the EPSRC National Facility for XPS operated by Cardiff University and University College, London under contract PR16195. The CCI Electron Microscopy facility was funded, in part, by the European Regional Development Fund through the Welsh Government and the Wolfson Foundation.

References

- Catalysing change, Defossilising the chemical industry, <https://royalsociety.org/news-resources/projects/defossilising-chemicals/>, accessed 17 September, 2025.
- W. Zhang, P. Zhang, H. Wang, J. Li and S. Y. Dai, *Trends Biotechnol.*, 2022, **40**, 1519.
- C. Hepburn, E. Adlen, J. Beddington, E. A. Carter, S. Fuss, N. MacDowell, J. C. Minx, P. Smith and C. K. Williams, *Nature*, 2019, **575**, 87.
- B. Long, F. Zhang, S. Y. Dai, M. Foston, Y. J. Tang and J. S. Yuan, *Nat. Rev. Bioeng.*, 2025, **3**, 230.
- R. A. Sheldon and A. C. S. Sus, *Chem. Eng.*, 2018, **6**, 4464.
- M. G. Davidson, S. Elgie, S. Parsons and T. J. Young, *Green Chem.*, 2021, **23**, 3154.
- X. Ji, Y. Lu and X. Chen, *Chem. Commun.*, 2025, **61**, 1303.
- X. Ji, Y. Zhao, M. Y. Lui, L. T. Mika and X. Chen, *iScience*, 2024, **27**, 109857.
- X. Chen, H. Yang and N. Yan, *Chem. Eur J.*, 2016, **22**, 13402–13421.
- J. Hou, B. E. Aydemir and A. G. Dumanli, *Philos. Trans. R. Soc., A*, 2021, **379**, 20200331.
- R. Cohen-Kupiec and I. Chet, *Curr. Opin. Biotechnol.*, 1998, **9**, 270.
- I. Tews, A. Perrakis, A. Oppenheim, Z. Dauter, K. S. Wilson and C. E. Vorgias, *Nat. Struct. Biol.*, 1996, **3**, 638.
- A. Munzone, V. G. H. Eijsink, J. G. Berrin and B. Bissaro, *Nat. Rev. Chem.*, 2024, **8**, 106.
- W. T. Beeson, V. V. Vu, E. A. Span, C. M. Phillips and M. A. Marletta, *Annu. Rev. Biochem.*, 2015, **84**, 923.
- B. Bissaro and V. G. H. Eijsink, *Essays Biochem.*, 2023, **67**, 575.
- G. Vaaje-Kolstad, B. Westereng, S. J. Horn, C. Liu, H. Zhai, M. Sørli and V. G. H. Eijsink, *Science*, 2010, **330**, 219.
- B. Bissaro, Å. K. Røhr, G. Müller, P. Chylenski, M. Skaugen, Z. Forsberg, S. J. Horn, G. Vaaje-Kolstad and V. G. H. Eijsink, *Nat. Chem. Biol.*, 2017, **13**, 1123.
- B. O. Burek, S. Bormann, F. Hollman, J. Z. Bloh and D. Holtmann, *Green Chem.*, 2019, **21**, 3232.
- K. Seelbach, M. P. J. van Deurzen, F. van Ranwijk, R. A. Sheldon and U. Kragl, *Biotechnol. Biofuels*, 1997, **55**, 283.
- G. Goor, J. Klenneberg, S. Jacobi, J. Dadabhoy and E. Candido, in *Ullmann's Encyclopedia of Industrial Chemistry*, ed. C. Ley, Wiley-VCH, Weinheim, 8th edn, 2019, p. 1.
- F. Tieves, S. J.-P. Willot, M. M. C. H. van Schie, M. C. R. Rauch, S. H. Younes, W. Zhang, J. Dong, P. G. de Santos, J. M. Robbins, B. Bommarius, M. Alcalde, A. S. Bommarius and F. Hollmann, *Angew. Chem., Int. Ed.*, 2019, **58**, 7873.
- Y. Ma, Y. Li, S. Ali, P. Li, W. Zhang, M. C. R. Rauch, S. J.-P. Willot, D. Ribitsch, Y.-H. Choi, M. Alcalde, F. Hollmann and Y. Wang, *ChemCatChem*, 2020, **12**, 989.
- D. I. Perez, M. M. Grau, I. W. C. E. Arends and F. Hollmann, *Chem. Commun.*, 2009, 6848.
- D. Holtman, T. Krieg, L. Getrey and J. Schrader, *Catal. Commun.*, 2014, **51**, 82.
- D. Jung, C. Streb and M. Hartmann, *Microporous Mesoporous Mater.*, 2008, **113**, 523529.
- S. J. Freakley, S. Kochius, J. van Marwijk, C. Fenner, R. J. Lewis, K. Baldenius, S. S. Marais, D. J. Opperman, S. T. L. Harrison, M. Alcalde, M. S. Smit and G. J. Hutchings, *Nat. Commun.*, 2019, **10**, 4178.
- J. Brehm, R. J. Lewis, T. Richards, T. Qin, D. J. Morgan, T. E. Davies, L. Chen, X. Liu and G. J. Hutchings, *ACS Catal.*, 2022, **12**, 11776.
- A. Stenner, R. J. Lewis, J. Brehm, T. Qin, A. López-Martin, D. J. Morgan, T. E. Davies, L. Chen, X. Liu and G. J. Hutchings, *ChemCatChem*, 2023, **15**, e202300162.
- J. K. Edwards, S. J. Freakley, A. F. Carley, C. J. Kiely and G. J. Hutchings, *Acc. Chem. Res.*, 2014, **47**, 845.
- A. Paradisi, E. M. Johnston, M. Tovborg, C. R. Nicoll, L. Ciano, A. Dowle, J. McMaster, Y. Hancock, G. J. Davies and P. H. Walton, *J. Am. Chem. Soc.*, 2019, **141**, 18585.
- M. Torbjörsson, M. Hagemann, U. Ryde and E. D. Hedegård, *J. Biol. Inorg. Chem.*, 2023, **28**, 317.
- S. Kuusk, V. G. H. Eijsink and P. Våljamäe, *J. Biol. Chem.*, 2023, **299**, 105094.
- A. Munzone, M. Pujol, A. Tamhankar, C. Joseph, I. Mazurenko, M. Réglie, S. A. V. Jannuzzi, A. Royant, G. Sicoli, S. DeBeer, M. Orio, A. J. Simaan and C. Decroos, *Inorg. Chem.*, 2024, **63**, 11063.
- B. Bissaro, B. Streit, I. Isaksen, V. G. H. Eijsink, G. T. Beckham, J. L. DuBois and Å. K. Røhr, *Proc. Natl. Acad. Sci. USA*, 2020, **117**, 1504.
- G. Vaaje-Kolstad, D. R. Houston, A. H. K. Riemen, V. G. H. Eijsink and D. M. F. van Aalten, *J. Biol. Chem.*, 2005, **280**, 11313.
- S. Kuusk, B. Bissaro, P. Kuusk, Z. Forsberg, V. G. H. Eijsink, M. Sørli and P. Våljamäe, *J. Biol. Chem.*, 2018, **293**, 523.
- C. M. Phillips, W. T. Beeson IV, J. H. Cate and M. A. Marletta, *ACS Chem. Biol.*, 2011, **6**, 1399.
- M. Sankar, Q. He, M. Morad, J. Pritchard, S. J. Freakley, J. K. Edwards, S. H. Taylor, D. J. Morgan, A. F. Carley, D. W. Knight, C. J. Kiely and G. J. Hutchings, *ACS Nano*, 2012, **6**, 6600.
- T. M. Hedison, E. Breslmayr, M. Shanmugam, K. Karnpakdee, D. J. Heyes, A. P. Green, R. Ludwig, N. S. Scrutton and D. Kracher, *FEBS J.*, 2021, **288**, 4115.
- V. G. H. Eijsink, D. Petrovic, Z. Forsberg, S. Mekasha, Å. K. Røhr, A. Várnai, B. Bissaro and G. Vaaje-Kolstad, *Biotechnol. Biofuels*, 2019, **12**, 58.
- A. Stepnov, Z. Forsberg, M. Sørli, G.-S. Nguyen, A. Wentzel, Å. K. Røhr and V. G. H. Eijsink, *Biotechnol. Biofuels*, 2021, **14**, 28.



- 42 O. Golten, I. Ayuso-Fernández, K. R. Hall, A. A. Stepnov, M. Sørli, Å. K. Røhr and V. G. H. Eijssink, *FEBS Lett.*, 2023, **597**, 1363.
- 43 R. J. Lewis and G. J. Hutchings, *ChemCatChem*, 2019, **11**, 298.
- 44 J. A. Bauer, M. Zamocká, J. Majtán and V. Bauerová-Hlinková, *Biomolecules*, 2022, **12**, 427.
- 45 N. H. Hoang, O. Golten, Z. Forsberg, V. G. H. Eijssink and M. Richter, *ChemBioChem*, 2023, **24**, e202300363.
- 46 S. Mekasha, I. R. Byman, C. Lynch, H. Toupalová, L. Andéra, T. Næs, G. Vaaje-Kolstad and V. G. H. Eijssink, *Process Biochem.*, 2017, **56**, 132.
- 47 G. Müller, P. Chylenski, B. Bissaro, V. G. H. Eijssink and S. J. Horn, *Biotechnol. Biofuels*, 2018, **11**, 209.
- 48 J. Brehm, R. J. Lewis, D. J. Morgan, T. E. Davies and G. J. Hutchings, *Catal. Lett.*, 2022, **152**, 254.
- 49 A. Stemmer, R. J. Lewis, J. Pask, D. J. Morgan, T. Davies and G. J. Hutchings, *Green Chem.*, 2026, **28**, 1586–1600.
- 50 N. M. Wilson and D. W. Flaherty, *J. Am. Chem. Soc.*, 2016, **138**, 574.
- 51 X. Gong, R. J. Lewis, S. Zhou, D. J. Morgan, T. E. Davies, x. Liu, C. J. Kiely, B. Zong and G. J. Hutchings, *Catal. Sci. Technol.*, 2020, **10**, 4635.
- 52 J. M. Campos-Martin, G. Blanco-Brieva and J. L. G. Fierro, *Angew. Chem., Int. Ed.*, 2006, **45**, 6962.
- 53 G. Gao, Y. Tian, X. Gong, Z. Pan, K. Yang and B. Zong, *Chin. J. Catal.*, 2020, **41**, 1039.
- 54 B. R. Scott, H. Z. Huang, J. Frickman, R. Halvorsen and K. S. Johansen, *Biotechnol. Lett.*, 2016, **38**, 425.

